Frequency Diverse Array Antenna: New Opportunities

Wen-Qin Wang

School of Communication and Information Engineering,
University of Electronic Science and Technology of China, Chengdu 610054, China
E-mail: wqwang@uestc.edu.cn

Imperial College London, London SW7 2AZ, U.K.

Abstract

Phased-array antennas are known for their capability to electronically steer a beam with high effectiveness, but beam steering is fixed in an angle for all range cells. This paper reviews frequency diverse array (FDA) antennas. Different from a phased array, an FDA uses a small frequency increment, as compared with the carrier frequency, across array elements. The use of a frequency increment generates an array factor that is a function of the angle, the time, and the range, allowing the FDA antenna to transmit the energy over the desired range and angle. In addition to analyzing FDA factor characteristics, this paper investigates FDA potential applications in range-dependent energy control and technical challenges in system implementation, with an aim to call for further investigations on the FDA.

Keywords: Arrays; array signal processing; frequency diverse array (FDA); range dependent; beamforming; phased array

1. Introduction

Phased-array antennas are known for their capability to electronically steer a beam with high effectiveness [1–3]. The directional gain offered by a phased-array antenna is useful for detecting/tracking weak targets and nulling interferences from other directions [4–7]. However, a limitation of a phased-array antenna is that the beam steering is independent of the range. Furthermore, the ability to control the range-dependent transmit energy distribution becomes an increasingly desirable trait in some applications [8–11], e.g., range-dependent interferences suppression, directional communications, and range ambiguities suppression. Although techniques exist to assist in mitigating range-dependent interferences, such as the space–time adaptive processing technique [12–16], they have a high computational cost. On the other hand, the desire for new and more advanced array antennas is driven by the requirements of many emerging applications ranging from multitask radar [17] to radio astronomy [18] and relay communication systems [19, 20].

Frequency diverse array (FDA) is a new concept proposed by Antonik et al. [21]–25]. An FDA uses a small frequency increment, as compared with the carrier frequency, across array elements. The frequency increment results in a range-dependent beampattern for which the beam focus direction will change as a function of the range, the angle, and the time [26–29]. Therefore, instead of angle-dependent beampatterns such as phased arrays, FDA patterns also depend on the frequency, the range, and the time, which could be exploited in radar applications. The FDA is different from the orthogonal frequency-division multiplexing (OFDM) technique [30, 31] and the multiple-input–multiple-output (MIMO) technique [32, 33]. OFDM uses orthogonal subcarriers, but nonorthogonal carriers are employed in the FDA. The MIMO technique uses signals collected from widely separated antennas to provide spatial diversity [34] or utilizes waveform diversity to increase the signal-to-noise ratio [35], whereas the FDA transmits the overlapping signals closely spaced in the frequency to provide a range-dependent beampattern for new functions. The FDA is also different from the conventional frequency scanning technique [36–39]. In a frequency scanning array, each element has the same frequency at a given time unlike the FDA [40].

Two FDA patents discussing range-dependent characteristics have been issued [24, 25]. The time and angle periodicity of an FDA beampattern is analyzed in [26]. A linear FDA is proposed in [41] for forward-looking-radar ground moving target indication (MTI). The application of the FDA in bistatic radar is studied in [42], and the application of a linear

Digital Object Identifier 10.1109/MAP.2015.2414692
Date of publication: 17 April 2015

frequency-modulated continuous waveform (LFMCW) for FDA systems is exploited in [43]. The phases of the FDA-transmitted signals constructively add in certain regions of space, whereas they destructively add in others. The range-dependent beampattern characteristics are extensively investigated in 26 and [44–48]. A full-wave simulation of an FDA antenna using the finite-difference time-domain method is proposed in [49], where the characteristics of a radiation pattern were investigated by each different simulation for the frequency offset change, the radiation element space change, and the array number change. In [43], the mathematical foundations of the LFMCW FDA are developed and used to design a basic proof-of-concept structure. Furthermore, the multipath characteristics of the FDA over a ground plane are analyzed in [50]. Additional work was reported in [51]–[54] to exploit the benefit of applying the FDA for synthetic aperture radar (SAR) high-resolution imaging.

Since the FDA apparent scan angle is not equal to the nominal scanning angle, precise beam steering depends on both the range and the angle. Consequently, it is not sufficient to precisely steer the beam similar to conventional phased arrays; nevertheless, the FDA provides new degrees of freedom in the range, the angle, and the time for designing and controlling the array factor [55]. This enables the array beam to scan without the need of phase shifters or mechanical steering because the array factor depends on the range and time variables. The auto-scanning property of the FDA was investigated in [26, 56], and [57]. In this paper, we introduce FDA potential applications and technical challenges, and we appeal to the antenna and propagation community for more publications and support on FDA research and development.

The remaining sections are organized as follows. Section 2 introduces the basic FDA scheme. Section 3 analyzes the FDA beampattern characteristics. Next, Section 4 discusses the new opportunities provided by the FDA in the range-dependent transmit energy control, the range-dependent interference suppression, and the range-dependent-only beampattern. Section 5 discusses several remaining problems. Finally, the conclusion is made in Section 6.

2. Basic FDA Scheme

Figure 1 illustrates a uniform linear array (ULA) FDA. Each FDA element radiates an incremental carrier frequency.

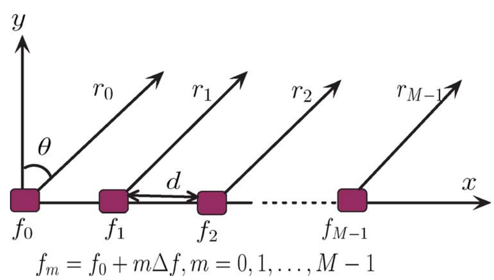

Figure 1. ULA FDA with frequency increment Δf.

That is, the monochromatic signal transmitted from the mth element can be expressed as

$$s_m(t) = \exp(j2\pi f_m t) \tag{1}$$

where radiation frequency f_m is

$$f_m = f_0 + m\Delta f, \qquad m = 0, 1, \ldots, M-1 \tag{2}$$

with f_0, Δf, and M being the carrier frequency, the frequency increment, and the number of array elements, respectively. The signal arriving at a given far-field point target (θ, r) (θ and r denote the azimuth angle and the slant range for the first element, respectively) is given by

$$s_m\left(t - \frac{r_m}{c_0}\right) = \exp\left\{j2\pi f_m\left(t - \frac{r_m}{c_0}\right)\right\} \tag{3}$$

where c_0 denotes the speed of light. The distance between the mth element and the target is

$$r_m = r - md\sin\theta, \qquad m = 0, 1, \ldots, M-1 \tag{4}$$

where d is the interelement spacing.

Suppose that the element factor can be factored out in the transmit field when the uniform transmit weight vector is employed in the FDA; in a narrow-band case, the array factor at position (θ, r) can be expressed as [42]

$$\begin{aligned} &\mathrm{AF}(t;\theta,r) \\ &= \sum_{m=0}^{M-1} \frac{1}{r_m} \exp\left\{j2\pi f_m\left(t - \frac{r_m}{c_0}\right)\right\} \\ &\approx \frac{\exp\left\{j2\pi f_0\left(t - \frac{r}{c_0}\right)\right\}}{r} \\ &\quad \times \sum_{m=0}^{M-1} \exp\left\{j2\pi\left(m\Delta f t - m\frac{\Delta f r}{c_0} + m\frac{df_0\sin\theta}{c_0}\right.\right. \\ &\qquad \left.\left. + m^2\frac{\Delta f d\sin\theta}{c_0}\right)\right\}. \end{aligned} \tag{5}$$

Although a general closed form of the array factor cannot be written, an approximate closed-form expression exists when $(M-1)\Delta f \ll f_0$. In [42], an approximate closed-form expression is obtained by ignoring term $m^2\Delta f d\sin\theta/c_0$. To investigate its reasonability, we can use an empirical phase requirement on the m^2 term as follows:

$$\frac{m^2\Delta f d\sin\theta}{c_0} < \frac{\pi}{4}. \tag{6}$$

As $m^2 \le (M-1)^2/2$ and $|\sin\theta| \le 1$, (6) can be equivalently written as

$$\Delta f < \frac{\pi c_0}{2(M-1)^2 d} \quad \text{or} \quad \frac{\Delta f}{f_0} < \frac{\pi c_0}{2(M-1)^2 d f_0}. \tag{7}$$

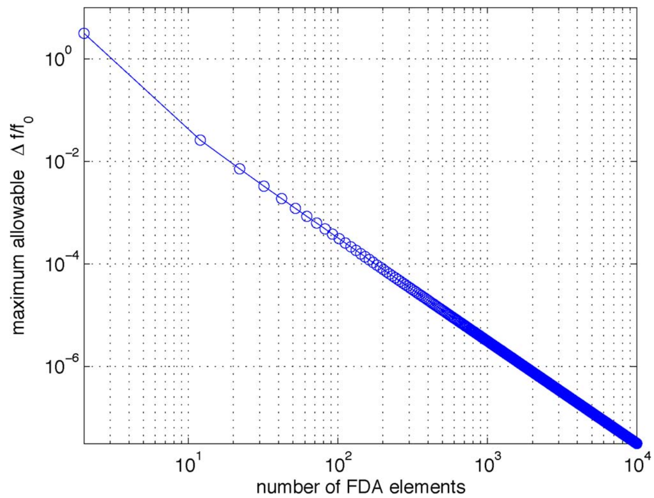

Figure 2. Maximum allowable fractional bandwidth $\Delta f/f_0$ versus the number of array elements.

On the other hand, since at a given time the frequency of each element is different from each other because of the frequency increment, to avoid the transmitted signal decorrelation in each element, the frequency increment is also limited by

$$\Delta f < \frac{1}{(M-1)T_c} \tag{8}$$

where T_c is the coherent processing time.

Suppose that $d = \lambda/2$, with λ being the wavelength, and $f_0 = 10$ GHz. Figure 2 gives the maximum allowable fractional bandwidth $\Delta f/f_0$ as a function of the number of array elements. It is noticed that, for a large-scale FDA, the approximation is only reasonable when a small fractional bandwidth is employed. To overcome this problem, we can replace term $m^2\Delta fd\sin\theta/c_0$ by $m\Delta fd\sin\theta/c_0$. In this case, (5) can be approximated as

$$\mathrm{AF}(t;\theta,r) \approx \frac{\exp\{j\Phi_0\}}{r}\frac{\sin\left[M\pi\left(\Delta ft - \frac{\Delta fr}{c_0} + \frac{df_0\sin\theta}{c_0} + \frac{\Delta fd\sin\theta}{c_0}\right)\right]}{\sin\left[\pi\left(\Delta ft - \frac{\Delta fr}{c_0} + \frac{df_0\sin\theta}{c_0} + \frac{\Delta fd\sin\theta}{c_0}\right)\right]}. \tag{9}$$

The additional phase factor Φ_0 is

$$\Phi_0 = 2\pi f_0\left(t - \frac{r}{c_0}\right) - \pi(M-1)\frac{\Delta fr}{c_0} + \pi(M-1)\frac{f_0 d\sin\theta}{c_0} + \pi(M-1)\frac{\Delta fd\sin\theta}{c_0} + \pi(M-1)\Delta ft. \tag{10}$$

3. FDA Factor Characteristics

3.1 Range-Dependent Array Factor

According to (5), Figure 3 shows the numerical transmit beampattern, where $\Delta f = 3$ kHz, $M = 12$, $f_0 = 10$ GHz, $d = \lambda/2$, and continuous-wave signals are assumed. Note that the unit of the scale is decibels. The regularity of the array factor as a function of the range and the angle is shown clearly. This is different from that of a conventional phased array. Since the arguments in the round brackets of (9) can be rearranged as

$$\Delta f\left(t - \frac{r}{c_0} + \frac{df_0\sin\theta}{\Delta fc_0} + \frac{d\sin\theta}{c_0}\right). \tag{11}$$

the difference between the peaks of the array factor at $\theta = 0$ and $\theta = \pi/2$ is $(c_0/\Delta f)(d/\lambda_0) + d$ in the range. Therefore, the shown "S"-shape of the array factor is a function of ratio d/λ_0 and of frequency increment Δf. Moreover, if the frequency increment is negative, the S-shaped amplitude of the array factor in Figure 3 will flip as well, as if the positive frequency increment is applied starting from the last toward the first element [42].

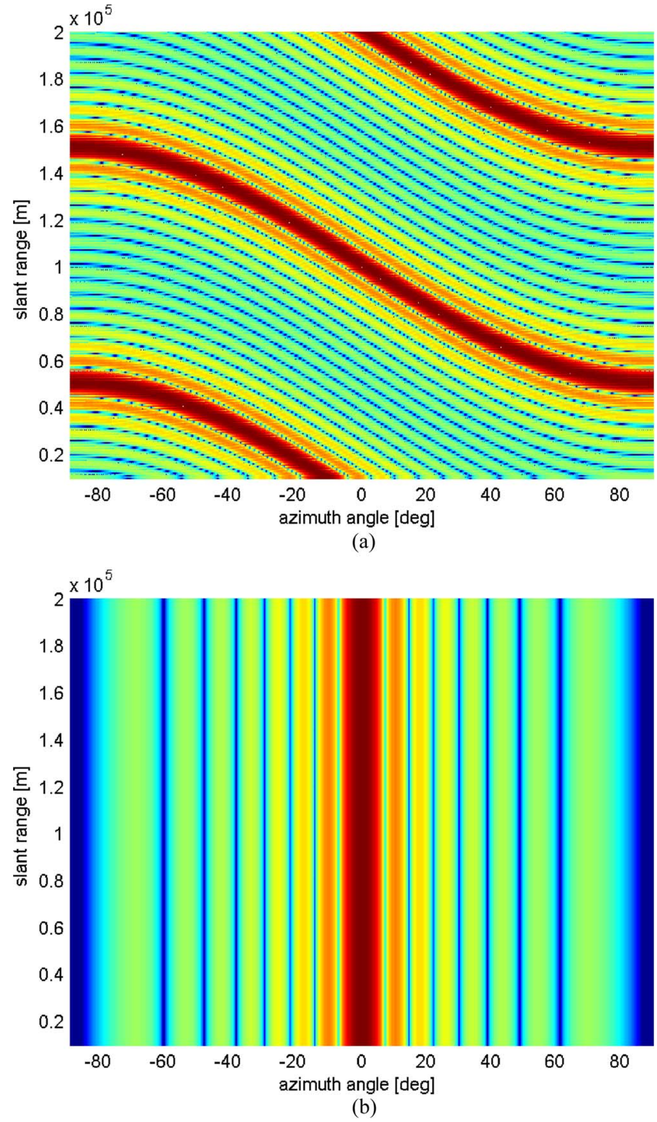

Figure 3. Comparison between the FDA and phased-array beampatterns, where $\Delta f = 3$ kHz, $M = 12$, $f_0 = 10$ GHz, and $d = \lambda/2$. (a) FDA beampattern. (b) Phased-array beampattern.

3.2 Periodicity of Array Factor

In (9), the maximum field is obtained when

$$\Delta f t - \frac{\Delta f r}{c_0} + \frac{d f_0 \sin\theta}{c_0} + \frac{\Delta f d \sin\theta}{c_0} = k \qquad k = 0, \pm 1, \pm 2, \ldots \quad (12)$$

This means that, when only one parameter is fixed, there are multiple solutions for the unfixed parameters. On the other hand, when two parameters are fixed, the pattern periodicity depends on the unfixed variable.

If (12) is solved for time t, we then have [29]

$$t = \frac{k}{\Delta f} + \frac{r}{c_0} - \frac{d f_0 \sin\theta}{c_0 f_0 \Delta f} - \frac{d \sin\theta}{c_0}. \quad (13)$$

This implies the periodic nature of the array factor in time. When range r and angle θ are fixed, the fundamental period is $1/\Delta f$. Suppose that $M = 10$, $r = 10$ km, $f_0 = 100$ MHz, $\theta = 0°$, and $\Delta f = 10$ kHz; Figure 4 shows the array factor when range $r = 10$ km and angle $\theta = 0°$ are fixed.

In the same manner, solving for range r yields

$$r = c_0 t + \frac{d f_0 \sin\theta}{\Delta f} - \frac{k c_0}{\Delta f} + d \sin\theta. \quad (14)$$

It reveals that the array factor is also a periodic function of the range assuming that both θ and t are fixed, as shown in Figure 5, where $M = 10$, $f_0 = 100$ MHz, $t = 250$ μs, $\theta = 0°$, and $\Delta f = 10$ kHz are assumed.

Similarly, if (12) is solved for $\sin\theta$, we can obtain

$$\sin\theta = \frac{k c_0 - \Delta f (c_0 t - r)}{d f_0 + \Delta f d}. \quad (15)$$

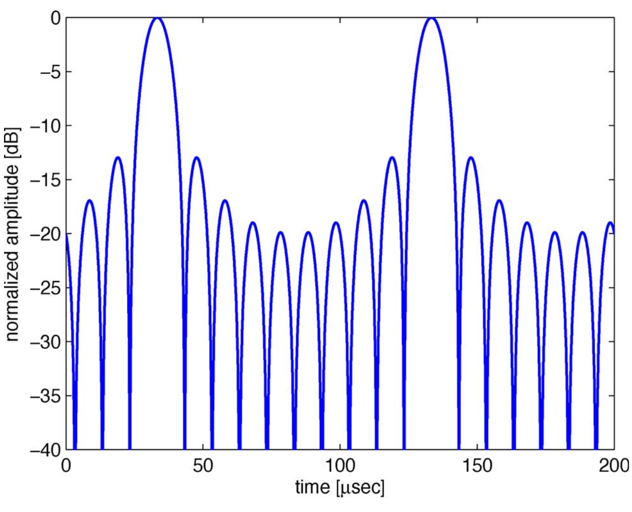

Figure 4. Array factor when range $r = 10$ km and angle $\theta = 0°$ are fixed.

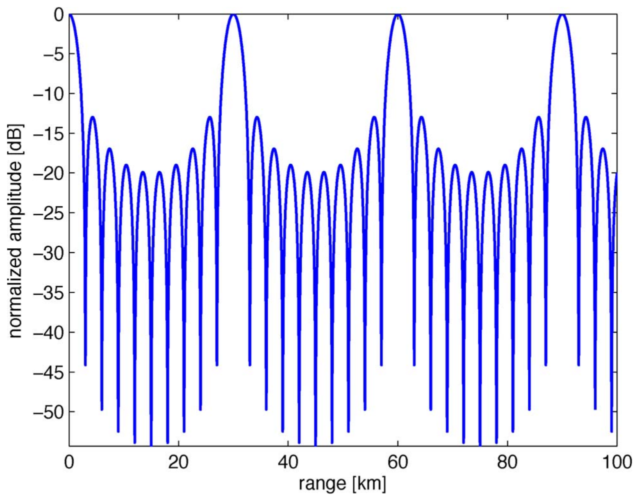

Figure 5. Array factor when time $t = 250$ and angle $\theta = 0°$ are fixed.

Obviously, $\sin\theta$ depends on both the time and range variables. This means that the FDA has an autoscanning property. Suppose that $M = 10$, $f_0 = 100$ MHz, $\theta = 0°$, and $\Delta f = 10$ kHz; Figure 6 shows the scanning angle at $t = 230$ μs and $t = 250$ μs.

4. New Opportunities

The FDA creates a range-dependent beampattern whose amplitude and spatial distribution can be controlled by the frequency increments and the number of array elements. Although the FDA cannot eliminate grating lobes totally, the grating lobes will be also range dependent. This provides a possibility to control the transmitted energy distribution or suppress/detect range-dependent interferences/targets.

4.1 Range-Dependent Transmit Beamforming

A frequency-coding technique can be employed for the FDA at the subarray level. We can divide the FDA into multiple subarrays that can be disjoint or overlapped [58], as shown in Figure 7. Each subarray uses a distinct frequency

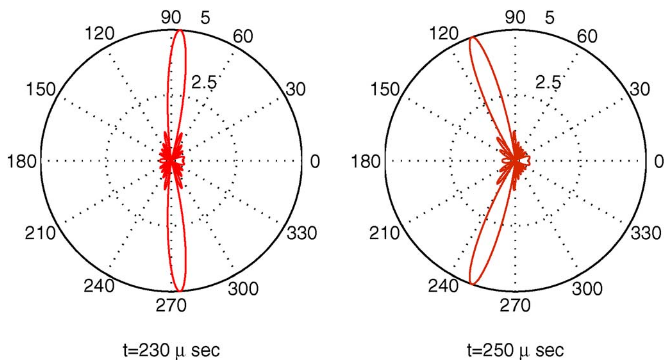

Figure 6. Scanning angles at $t = 230$ μs and $t = 250$ μs.

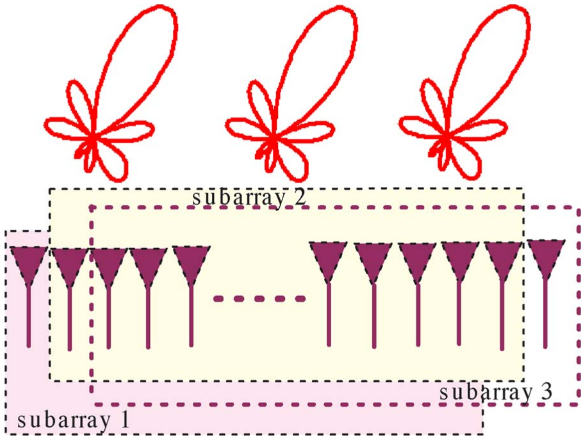

Figure 7. Illustration of the FDA transmit beamforming.

increment and forms a directional beam. All beams are steerable by tuning the frequency increments.

When the frequency-coding technique is employed, the signal transmitted by the *m*th element for the *k*th beam can be modeled as

$$s_{km}(t) = \gamma_k(t)\exp(j2\pi f_{km}t) \tag{16}$$

where $\gamma_k(t)$ are the frequency-coding sequences, and $f_{km} = f_0 + m\Delta f_k$, $m = 0, 1, \ldots, M-1$, with Δf_k being the frequency increment used in the *k*th beam. If we steer the *k*th beam to range r_k and angle θ_k, the composite *K*-beam pattern is given by [59]

$$s_T(t) = \sum_{k=1}^{K}\sum_{m=0}^{M-1}\gamma_k\left(t - \frac{r_k}{c_0} + \frac{md\sin\theta_k}{c_0}\right) \times \exp\left\{j2\pi f_{km}\left(t - \frac{r_k}{c_0} + \frac{md\sin\theta_k}{c_0}\right)\right\} \tag{17}$$

Consider an X-band two-subarray FDA with carrier frequency $f_0 = 10$ GHz and frequency increments $\Delta f_1 = 30$ kHz and $\Delta f_2 = 10$ kHz. We consider a linear FDA with 20 elements. The array is divided into two equal subarrays, and each subarray uses a distinct frequency-coding sequence. Suppose that the array direction angle is $\theta_0 = 10°$ and that the range is $r_0 = 10$ km; Figure 8 shows an array factor comparison between the basic and frequency-coding FDAs. Different from the basic FDA, the frequency-coding FDA shown also has a range resolution.

Since the direction and amount of focus can be determined analytically, multiple targets at different ranges or angles can be illuminated simultaneously. This provides a potential to multipath mitigation. Multipath occurs because the signals reflected from scatterers at different range cells have varying round-trip delays. The signals coherently add in the receiver, producing a resultant sum signal that has a longer duration than the direct path signal alone. By applying the FDA that focuses in different directions as a function of the range, the phase coherency of the multipath components can be disturbed such that the resultant sum is less dispersive. Furthermore, a

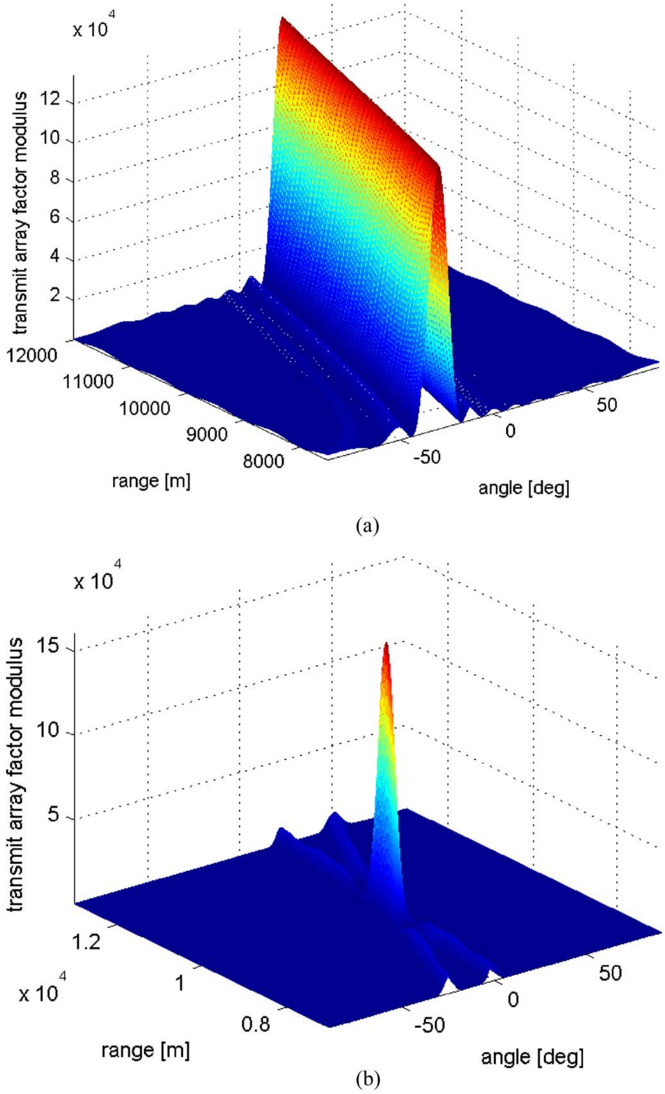

Figure 8. Comparison between the basic and frequency-coding FDA factors. (a) Basic FDA. (b) Frequency-coding FDA.

more sophisticated frequency-coding strategy may enable the development of multiple operation modes that support simultaneous SAR and MTI through a single antenna [27].

4.2 Range-Dependent-Only Beampattern

In order to eliminate the coupling between the range and the angle in the array factor expression, the array elements can be arranged in different configurations [42]. The essence is to make the distances d_m to a virtual reference point (which is fixed for the system) proportional to λ_m as

$$d_m = L\lambda_m, \quad m = 0, 1, \ldots, M-1. \tag{18}$$

Constant L should be big enough to ensure that the spacing between any two adjacent elements, i.e.,

$$\Delta d_m = L(\lambda_{m-1} - \lambda_m) \tag{19}$$

can be feasible in hardware manufacturing. Note that, despite the high value of L, spacing Δd_m is approximately equal to $L(\lambda_{M-2} - \lambda_{M-1})$.

In this case, the array factor can be written as [42]

$$\begin{aligned} \mathrm{AF}(t;\theta,r) &= \sum_{m=0}^{M-1} \frac{1}{r_m} \exp\left\{-j2\pi\left(f_m t - \frac{r_m}{\lambda_m}\right)\right\} \\ &\approx \frac{1}{r}\sum_{m=0}^{M-1} \exp\left\{-j2\pi L \sin\theta - j2\pi f_m\left(t - \frac{r}{c_0}\right)\right\} \\ &= \frac{\exp\left\{-j2\pi\left[L\sin\theta + f_0\left(t-\frac{r}{c_0}\right)\right]\right\}}{r} \\ &\quad \times \frac{\sin\left[M\pi\Delta f\left(t-\frac{r}{c_0}\right)\right]}{\sin\left[\pi\Delta f\left(t-\frac{r}{c_0}\right)\right]}. \end{aligned} \tag{20}$$

Equation (20) reveals that the angle dependence is found in the phase term only, whereas the amplitude depends on the time, the range, and the frequency increment only and no longer on the angle. It can be observed in Figure 9 that the array factor exhibits a constant peak gain with the angle at a particular range. This unusual beampattern can be used for suppressing range-dependent interferences.

5. Remaining Problems

The FDA provides many promising potentials, but there are several remaining problems as follows.

5.1 Waveform Optimization

Waveform optimization is required to further understand how the signal parameters affect the system performance. The ambiguity function may provide a useful optimization metric. Using the knowledge of the ambiguity function's primary sidelobe locations, an optimization algorithm could be designed to optimize the ambiguity function at those locations. The waveform can be designed by the optimization constraints, including the total bandwidth, the number of subcarriers, the number of transmit and receive elements, the maximum chirp rate, the maximum transmit signal amplitude, and the maximum peak sidelobe levels. This constrained optimization problem should be further investigated.

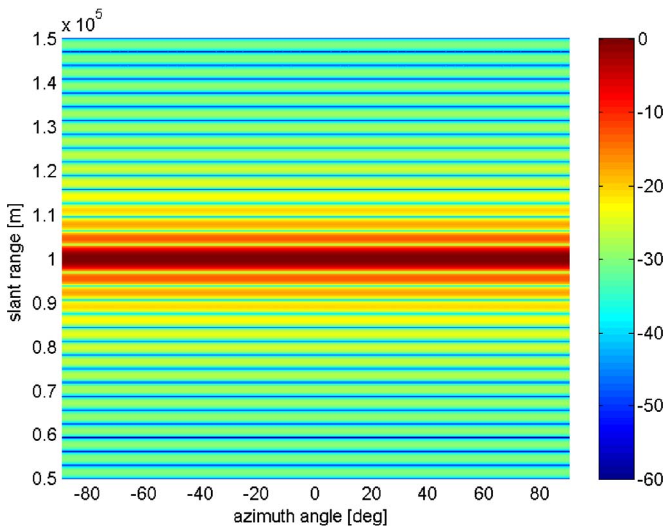

Figure 9. Range-dependent-only transmit–receive array factor, where $M = 10$, $\theta = 10^\circ$, $r = 100$ km, and $\Delta f = 3$ kHz are assumed.

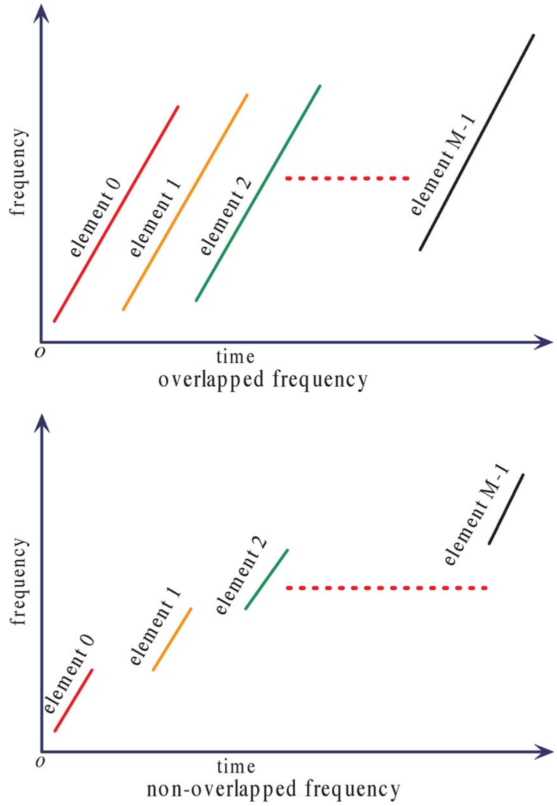

Figure 10. Two chirp implementations of an FDA system.

It is possible to use the FDA to transmit a chirp signal toward a desired direction at the transmitter while using a single carrier to demodulate the chirp signal at the receiver. This concept combines the flexible scanning feature of the FDA and the high-resolution imaging ability of the chirp signal. Figure 10 shows two chirp implementations of an FDA system. Particularly, we may utilize the contiguous and non-overlapping spectra on adjacent elements. This idea is similar to but different from a conventional frequency-stepped system. Using a contiguous bandwidth implementation, it may be possible to construct very large bandwidth signals, with each element radiating a nonoverlapping segment of the entire frequency extent. In this way, a higher range resolution may be obtained [53].

5.2 Array Configuration

Linear array geometry is exclusively used in literature because it allows the relationship between the temporal, spatial, and spectral aspects of the FDA to be clearly visualized.

However, a linear FDA does not perform well in target localization and 3-D imaging. On the other hand, planar geometry and even distributed FDA geometry are often required in actual applications. The FDA with constant element spacing may not be an ideal configuration due to the frequency diversity. Larger interelement spacing may be utilized to reduce the array complexity. Furthermore, we may consider nonlinear frequency increments for the FDA. An optimal FDA geometric configuration is thus a necessary future research work.

5.3 Optimal Array Processing

It is necessary to reduce the computation complexity in receiver signal processing. For example, the complex transmit–receive weighting functions depend on the baseband frequency and the frequency offset. Relaxing the weighting function's frequency offset dependence would allow the spatial weighting to be factored out from the summation and applied once to the entire signal. This can significantly reduce the computation complexity, but we found no related literature. On the other hand, the FDA's target detection and estimation performance should be evaluated in noise and clutter. Although a number of optimal processing techniques exist in literature for narrow-band and monochromatic signals, existing optimal techniques to process the FDA signal have not been studied. Additionally, more investigations should be performed for a receiver processing architecture [60] and implementation-specific problems, such as the generation of incremental carriers, phase synchronization, beamformer networks, antenna elements, digital processors, filters, etc. For instance, implementing the FDA concept on array hardware might require agile local oscillators and mixers to change the frequency for each element of the array.

6. Conclusion

This paper has reviewed an FDA antenna, which is of great interest for future communication, navigation, and radar applications. The range–angle-dependent array factor allows the FDA to transmit energy over a desired range or angle. This provides a potential to suppress range-dependent clutter and interference, which are not accessible for continuous-wave phased arrays (but it can be achieved with pulsed operation). The application potential of the FDA in range-dependent transmit beamforming and in a range-dependent-only transmit–receive beampattern is discussed, along with the technical challenges in waveform optimization, the array configuration, and optimal array processing.

7. Acknowledgment

This work was supported in part by the National Natural Science Foundation of China under grant 41101317, Program for New Century Excellent Talents in University under grant NCET-12-0095 and a Marie Curie Fellowship (FP7/2007-2013, grant agreement PIIF-GA-2012-326672).

8. References

[1] T. A. Lam, D. C. Vier, J. A. Nieslsen, C. G. Parazzoli, and M. H. Tanielian, "Steering phased array antenna beams to the horizon using a buckyball NIM lens," *Proc. IEEE*, vol. 99, no. 10, pp. 1755–1767, Oct. 2011.

[2] B. Bauman, A. Christianson, A. Wegener, and W. J. Chappell, "Dynamic visualization of antenna patterns and phased-array beam steering," *IEEE Antennas Propag. Mag.*, vol. 54, no. 3, pp. 184–193, Jun. 2012.

[3] C. J. Reddy, "Phased array-based systems and applications," *IEEE Antennas Propag. Mag.*, vol. 39, no. 5, pp. 102–103, Oct. 1997.

[4] P. Rocca, R. L. Haupt, and A. Massa, "Interference suppression in uniform linear arrays through a dynamic thinning strategy," *IEEE Trans. Antennas Propag.*, vol. 59, no. 12, pp. 4525–4533, Dec. 2011.

[5] F. Tokan and F. Gunes, "Interference suppression by optimizing the positions of selected elements using generalized pattern search algorithm," *IEEE Microw., Antennas Propag.*, vol. 5, no. 2, pp. 127–135, Jan. 2011.

[6] J. R. Mosig, "An old tool and a new challenge for depicting antenna array radiation patterns," *IEEE Antennas Propag. Mag.*, vol. 53, no. 3, pp. 115–123, Mar. 2011.

[7] T. F. Chun, A. Zamora, J. L. Bao, R. T. Iwami, and W. A. Shiroma, "An interleaved, interelement phase-detecting/phase-shifting retrodirective antenna array for interference reduction," *IEEE Antennas Wireless Propag. Lett.*, 2011, vol. 10, pp. 919–922.

[8] X. L. Jin, G. Y. Min, S. Velentzas, and J. M. Jiang, "Quality-of-service analysis of queuing systems with long-range-dependent network traffic and variable service capacity," *IEEE Trans. Wireless Commun.*, vol. 11, no. 2, pp. 562–570, Feb. 2012.

[9] J. X. Wu, T. Wang, L. F. Zhang, and Z. Bao, "Range-dependent clutter suppression for airborne sidelooking radar using MIMO technique," *IEEE Trans. Aerosp. Electron. Syst.*, vol. 48, no. 4, pp. 3647–3654, Oct. 2012.

[10] X. S. Yang, H. V. Poor, and A. P. Petropulu, "Memoryless discrete-time signal detection in long-range dependent noise," *IEEE Trans. Signal Process.*, vol. 52, no. 6, pp. 1607–1619, Jun. 2004.

[11] J. Li, G. S. Liao, and H. Griffiths, "Range-dependent clutter cancellation method in bistatic MIMO-STAP radars," in *Proc. CIE Int. Conf. Radar Dig.*, Chengdu, China, Oct. 24–27, 2011, pp. 59–62.

[12] T. K. Sarkar et al., "A deterministic least-squares approach to space-time adaptive processing (STAP)," *IEEE Trans. Antennas Propag.*, vol. 49, no. 1, pp. 91–103, Jan. 2001.

[13] M. M. Weiner, "Proposed algorithm for sequential implementation of adaptive antennas and receivers," *IEEE Antennas Propag. Mag.*, vol. 51, no. 5, pp. 161–162, May 2009.

[14] D. Cristallini and W. Burger, "A robust direct data domain approach for STAP," *IEEE Trans. Signal Process.*, vol. 60, no. 3, pp. 1283–1294, Mar. 2012.

[15] W. L. Melvin, "A STAP overview," *IEEE Aerosp. Electron. Syst. Mag.*, vol. 19, no. 1, pp. 19–35, Jan. 2004.

[16] M. Zatman, "Circular array STAP," *IEEE Trans. Aerosp. Electron. Syst.*, vol. 36, no. 2, pp. 510–517, Apr. 2000.

[17] V. Murthy, U. Pillai, and M. E. Davis, "Waveforms for simultaneous SAR and GMTI," in *Proc. IEEE Radar Conf. Dig.*, Atlanta, CA, USA, May 7–11, 2012, pp. 51–56.

[18] G. Oliveri, F. Caramanica, and A. Massa, "Hybrid ADS-based techniques for radio astronomy array design," *IEEE Trans. Antennas Propag.*, vol. 59, no. 6, pp. 1817–1827, Jun. 2011.

[19] S. Genovesi, A. Di Candia, and A. Monorchio, "Compact and low profile frequency agile antenna for multiband wireless communication systems," *IEEE Trans. Antennas Propag.*, vol. 62, no. 3, pp. 1019–1026, Mar. 2014.

[20] M. H. Shariat, M. Biguesh, and S. Gazor, "Signal-to-noise-ratio maximisation for linear multi-antenna relay communication," *IET Commun.*, vol. 8, no. 2, pp. 172–183, Jan. 2014.

[21] P. Antonik, M. C. Wicks, H. D. Griffiths, and C. J. Baker, "Frequency diverse array radars," in *Proc. IEEE Radar Conf. Dig.*, Verona, NY, USA, Apr. 24–27, 2006, pp. 215–217.

[22] P. Antonik, M. C. Wicks, H. D. Griffiths, and C. J. Baker, "Multi-mission multi-mode waveform diversity," in *Proc. IEEE Radar Conf. Dig.*, Verona, NY, USA, Apr. 24–27, 2006, pp. 580–582.

[23] P. Antonik and M. C. Wicks, "Method and apparatus for simultaneous synthetic aperture and moving target indication," U.S. Patent 20 080 129 584, Jun. 5, 2008.

[24] M. C. Wicks and P. Antonik, "Frequency diverse array with independent modulation of frequency, amplitude, and phase," U.S. Patent 7 319 427, Jan. 15, 2008.

[25] M. C. Wicks and P. Antonik, "Method and apparatus for a frequency diverse array," U.S. Patent 751 166 5B2, Mar. 31, 2009.
[26] M. Secmen, S. Demir, A. Hizal, and T. Eker, "Frequency diverse array antenna with periodic time modulated pattern in range and angle," in *Proc. IEEE Radar Conf. Dig.*, Boston, MA, USA, Apr. 17–20, 2007, pp. 427–430.
[27] P. Antonik, "An investigation of a frequency diverse array," Ph.D. dissertation, Univ. College London, London, U.K., 2009.
[28] A. Aytun, "Frequency diverse array radar," M.S. thesis, Naval Postgraduate School, Monterey, CA, USA, 2010.
[29] S. Brady, "Frequency diverse array radar: Signal characterization and measurement accuracy," M.S. thesis, Air Force Inst. Technol., Wright-Patterson AFB, OH, USA, 2010.
[30] W.-Q. Wang, "Mitigating range ambiguities in high PRF SAR with OFDM waveform diversity," *IEEE Geosci. Remote Sens. Lett.*, vol. 10, no. 1, pp. 101–105, Jan. 2013.
[31] R. F. Tigrek, W. J. A. D. Heij, and P. V. Genderen, "OFDM signals as the radar waveform to solve Doppler ambiguity," *IEEE Trans. Aerosp. Electron. Syst.*, vol. 48, no. 1, pp. 130–143, Jan. 2012.
[32] H. Liu, S. Gao, and T. H. Loh, "Compact MIMO antenna with frequency reconfigurability and adaptive radiation patterns," in *Proc. IEEE Antennas Wireless Propag. Lett.*, 2013, vol. 12, pp. 269–272.
[33] R. Mehmood and J. W. Wallace, "MIMO capability enhancement using parasitic reconfigurable aperture antennas (RECAPS)," *IEEE Trans. Antennas Propag.*, vol. 60, no. 2, pp. 665–673, Feb. 2012.
[34] A. M. Haimovich, R. S. Blum, and L. J. Cimini, "MIMO radar with widely separated antennas," *IEEE Signal Process. Mag.*, vol. 25, no. 1, pp. 116–129, Jan. 2008.
[35] J. Li and P. Stoica, "MIMO radar with colocated antennas," *IEEE Signal Process. Mag.*, vol. 24, no. 5, pp. 106–114, Sep. 2007.
[36] F. S. Johansson, L. G. Josefsson, and T. Lorentzon, "A novel frequency-scanned reflector antenna," *IEEE Trans. Antennas Propag.*, vol. 37, no. 8, pp. 984–989, Aug. 1989.
[37] L. Ranzani et al., "W-band micro-fabricated coaxially-fed frequency scanned slot arrays," *IEEE Trans. Antennas Propag.*, vol. 61, no. 4, pp. 2324–2328, Apr. 2013.
[38] A. Zandieh, A. S. Abdellatif, A. Taeb, and S. Safavi-Naeini, "Low-cost and high-efficiency antenna for millimeter-wave frequency-scanning applications," in *Proc. IEEE Antennas Wireless Propag. Lett.*, 2013, vol. 12, pp. 116–119.
[39] C. Vazquez, C. Garcia, Y. Alvarez, S. Ver-Hoeye, and F. Las-Heras, "Near-field characterization of an imaging system based on a frequency scanning antenna array," *IEEE Trans. Antennas Propag.*, vol. 61, no. 5, pp. 2874–2879, May 2013.
[40] E. D. Cullens et al., "Micro-fabricated 130–180 GHz frequency scanning waveguide arrays," *IEEE Trans. Antennas Propag.*, vol. 60, no. 8, pp. 3647–3653, Aug. 2012.
[41] P. Baizert, T. B. Hale, M. A. Temple, and M. C. Wicks, "Forward-looking radar GMTI benefits using a linear frequency diverse array," *Electron. Lett.*, vol. 42, no. 22, pp. 1311–1312, Oct. 2006.
[42] P. F. Sammartino, C. J. Baker, and H. D. Griffiths, "Frequency diverse MIMO techniques for radar," *IEEE Trans. Aerosp. Electron. Syst.*, vol. 49, no. 1, pp. 201–222, Jan. 2013.
[43] T. Eker, S. Demir, and A. Hizal, "Exploitation of linear frequency modulation continuous waveform (LFMCW) for frequency diverse arrays," *IEEE Trans. Antennas Propag.*, vol. 61, no. 7, pp. 3546–3553, Jul. 2013.
[44] P. Antonik, M. C. Wicks, H. D. Griffiths, and C. J. Baker, "Range dependent beamforming using element level waveform diversity," in *Proc. Int. Waveform Diversity Des. Conf. Dig.*, Las Vegas, NV, USA, Jan. 22–27, 2006, pp. 1–4.
[45] T. Higgins and S. Blunt, "Analysis of range-angle coupled beamforming with frequency diverse chirps," in *Proc. Int. Waveform Diversity Des. Conf. Dig.*, Orlando, FL, USA, Feb. 8–13, 2009, pp. 140–144.
[46] W.-Q. Wang, "Range-angle dependent transmit beampattern synthesis for linear frequency diverse arrays," *IEEE Trans. Antennas Propag.*, vol. 61, no. 8, pp. 4073–4081, Aug. 2013.
[47] L. Zhuang and X. Z. Liu, "Precisely beam steering for frequency diverse arrays based on frequency offset selection," in *Proc. Int. Radar Conf. Dig.*, Bordeaux, France, Oct. 12–16, 2009, pp. 1–4.
[48] Y. G. Chen, Y. T. Li, Y. H. Wu, and H. Chen, "Research on the linear frequency diverse array performance," in *Proc. Int. Signal Process. Conf. Dig.*, Beijing, China, Oct. 24–28, 2010, pp. 2324–2327.
[49] J. Shin et al., "Full-wave simulation of frequency diverse array antenna using the FDTD method," in *Proc. Asia-Pacific Microw. Conf. Dig.*, Seoul, Korea, Nov. 5–8, 2013, pp. 1070–1072.
[50] C. Cetinepe and S. Demir, "Multipath characteristics of frequency diverse arrays over a ground plane," *IEEE Trans. Antennas Propag.*, vol. 62, no. 7, pp. 3567–3574, Jul. 2014.
[51] J. Farooq, M. A. Temple, and M. A. Saville, "Application of frequency diverse arrays to synthetic aperture radar imaging," in *Proc. Int. Electromagn. Adv. Appl. Conf. Dig.*, Torino, Italy, Sep. 17–21, 2007, pp. 447–449.
[52] J. Farooq, M. A. Temple, and M. A. Saville, "Exploiting frequency diverse array processing to improve SAR imaging resolution," in *Proc. IEEE Radar Conf. Dig.*, Rome, Italy, May 26–30, 2008, pp. 1–5.
[53] J. Farooq, "Frequency diversity for improving synthetic aperture radar imaging," Ph.D. dissertation, Air Force Instit. Technol., Wright-Patterson AFB, OH, USA, 2009.
[54] W. Khan and I. M. Qureshi, "Frequency diverse array radar with time-dependent frequency offset," in *Proc. IEEE Antennas Wireless Propag. Lett.*, 2014, vol. 13, pp. 758–761.
[55] W.-Q. Wang, "Phased-MIMO radar with frequency diversity for range-dependent beamforming," *IEEE Sens. J.*, vol. 13, no. 4, pp. 1320–1328, Apr. 2013.
[56] S. Huang, K. F. Tong, and C. J. Baker, "Frequency diverse array: Simulation and design," in *Proc. LAPS Antennas Propag. Conf. Dig.*, Loughborough, U.K., May 16–17, 2009, pp. 253–256.
[57] S. Huang, K. F. Tong, and C. J. Baker, "Frequency diverse array with beam scanning feature," in *Proc. IEEE Antennas Propag. Conf. Dig.*, San Diego, CA, USA, Jul. 5–11, 2008, pp. 1–4.
[58] W.-Q. Wang and H. Z. Shao, "A flexible phased-MIMO array antenna with transmit beamforming," *Int. J. Antennas Propag.*, vol. 2012, Jan. 2012, pp. 1–10.
[59] A. M. Jones, "Frequency diverse array receiver architectures," Ph.D. dissertation, Wright State Univ., Dayton, OH, USA, 2011.
[60] A. M. Jones and B. D. Rigling, "Planar frequency diverse array receiver architecture," in *Proc. IEEE Radar Conf. Dig.*, Atlanta, GA, USA, May 7–11, 2012, pp. 145–150.

Wen-Qin Wang (M'08) received the B.S. degree in electrical engineering from Shandong University, Jinan, China, in 2002 and the M.E. and Ph.D. degrees in information and communication engineering from the University of Electronic Science and Technology of China (UESTC), Chengdu, China, in 2005 and 2010, respectively.

From March 2005 to March 2007, he was with the National Key Laboratory of Microwave Imaging Technology, Chinese Academy of Sciences, Institute of Electronics, Beijing, China. Since September 2007, he has been with the School of Communication and Information Engineering, UESTC, where he is currently a Professor. From June 2011 to May 2012, he was a Visiting Scholar with the Stevens Institute of Technology, Hoboken, NJ, USA. From December 2012 to December 2013, he was a Hong Kong Scholar with the City University of Hong Kong, Kowloon, Hong Kong. He is also currently a Marie Curie Fellow with Imperial College London, London, U.K. He is the author or coauthor of two books published by Springer and CRC Press, respectively. His research interests include communication and radar signal processing, and novel radar imaging techniques.

Dr. Wang is an editorial board member of four international journals. He was the recipient of the Marie Curie International Incoming Fellow, the Hong Kong Scholarship, the New Century Excellent Talents in University Award, a nomination award of the National Excellent Doctorate Dissertation of China, and the Distinguished Young Scholars of Sichuan Province Award.